Applied Catalysis B: Environmental 324 (2023) 122219

Contents lists available at ScienceDirect

Applied Catalysis B: Environmental

journal homepage: www.elsevier.com/locate/apcatb

# Catalytic conversion of model compounds of plastic pyrolysis oil over ZSM-5

Son Dong [a], Houqian Li [b], Iris K. Bloede [a], Abdullah J. Al Abdulghani [b], Edgard A. Lebrón-Rodríguez [b], George W. Huber [b], Ive Hermans [a,b,*]

[a] Department of Chemistry, University of Wisconsin-Madison, 1101 University Ave, Madison, WI, 53706, USA
[b] Department of Chemical and Biological Engineering, University of Wisconsin-Madison, 1415 Engineering Drive, Madison, WI, 53706, USA

ARTICLE INFO

*Keywords:*
Pyrolysis
Catalytic cracking
ZSM-5
Zeolite
Plastic

ABSTRACT

Mechanistic investigation of the catalytic conversion of model compounds for plastic pyrolysis oil (1-octene, octadiene, octane, and toluene) over ZSM-5 in a fixed-bed reactor was studied. 1-Octene breaks down into smaller olefins, which undergo further cracking, oligomerization, cyclization, and hydrogen transfer to eventually produce benzene, toluene, xylene (BTX), coke, and hydrogen. The effect of contact time on 1-octene conversion was further investigated and compared with thermodynamics analyses to elucidate the reaction network. Under the reaction conditions (500 °C, 1 atm), octadiene undergoes thermal coking, significantly contributing to reactor fouling. The products from octane cracking are similar to the products from 1-octene conversion whereas toluene undergoes disproportionation, dealkylation and coking. The analysis of spent catalyst showed long-chain hydrocarbons created by oligomerization reactions filled the pores and covered the surface of the catalyst. When mesoporous ZSM-5 is used instead of conventional, product selectivity is maintained for 70 h in time-on-stream experiments.

## 1. Introduction

The invention and large-scale deployment of polymers is one of the most important breakthroughs of the 20th century. However, despite being a wonderful invention that has improved our standard of living, plastic waste is an unsolved problem that needs to be addressed. Of the 6300 tons of plastic waste that were produced in 2015, only 9 % was recycled, 12 % was incinerated for energy generation, while the rest was disposed of in landfill or dumps [1]. Despite being the cheaper method to handle plastic waste, landfilling has led to pollution and ecological risks [2–4]. Pyrolysis is a technology to create oil from waste plastics. There has been significant investment in technologies to produce plastic pyrolysis oils [5]. The oil contains hydrocarbons ranging from 5 to 60 carbons in length with the main components being olefins, dienes, paraffins and aromatics [6]. Although the precise composition of pyrolysis oil depends on the plastic feedstock as well as the pyrolysis temperature, olefins always make up the majority of the products [6–13].

The plastic oils can be used as fuel or upgraded into aromatics and olefins that can then be used as new building-block chemicals. Steam cracking and catalytic cracking are two of the most promising routes for further utilization of the plastic pyrolysis oils. Plastic oil contains high concentrations of olefins and metal contaminants that exceed feedstock specifications used in steam crackers [7]. As the contaminants in the plastic pyrolysis oil may cause corrosion problems with the steam cracking equipment, only blends (typically less than 5 % plastic pyrolysis oils) are being studied [7]. In blends with naphtha for a steam cracker feed stream, primarily C2-C4 olefins and BTX are produced. The light naphtha fraction of the plastic pyrolysis oil can be upgraded directly by this route. The heavier fraction of plastic pyrolysis oil would have to undergo cracking (with or without hydrogen) to a light naphtha fraction before it could be used in a naphtha steam cracker as it does not have a similar boiling point as naphtha [9,14]. Zeolite upgrading could potentially be a single stand-alone unit to convert the plastic oils into aromatics and olefins [13,15]. Zeolites can also be integrated in a circulating fluidized bed plastic pyrolysis reactor to directly produce aromatics and olefins [16–18].

Numerous studies investigated zeolites to produce aromatics and short-chain olefins from olefins, the main product of plastic oil [19–36]. The advantage of using zeolites depends on the structure of the zeolite.

* Correspondence to: 1101 University Avenue Madison, Wisconsin 53706.
*E-mail address:* hermans@chem.wisc.edu (I. Hermans).

https://doi.org/10.1016/j.apcatb.2022.122219
Received 14 September 2022; Received in revised form 23 November 2022; Accepted 25 November 2022
Available online 26 November 2022

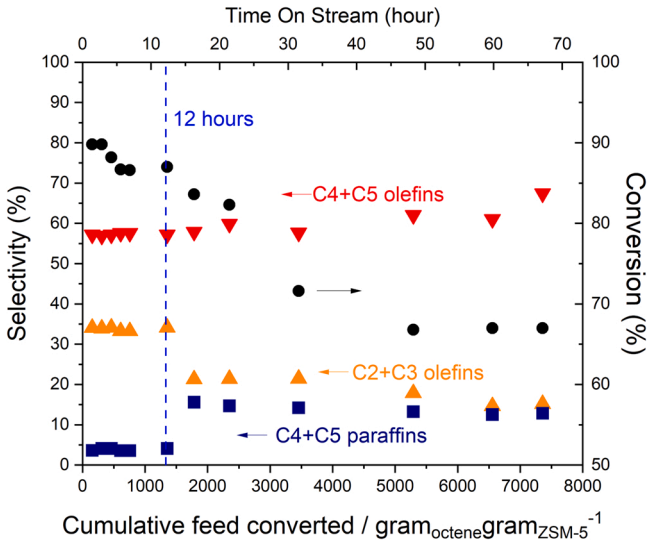


**Fig. 1.** Time-on-stream cracking of octene on ZSM-5 (reaction conditions: $m_{ZSM-5}$ = 10 mg, 500 °C, $P_{octene}$ = 4 kPa, $N_2$ = 140 mL min$^{-1}$, contact time = 9 ms).

**Table 1**
Summary of cracking of several model compounds (partial pressure of compound = 4 kPa, 500 °C, 1 g ZSM-5, contact time = 1.0 s).

| Feed | 1-Octene | Octane | Toluene | Octadiene |
|---|---|---|---|---|
| Conversion | 100 | 100 | 25.4 | 100 |
| ***Yield(%)*** | | | | |
| Methane | 5.1 ± 0.1 | 4.9 ± 0.3 | 0 | 1.5 |
| Ethane | 3.7 ± 0.4 | 6.4 ± 0.3 | 0 | 1.0 |
| Ethylene | 9.6 ± 0.4 | 8.4 ± 0.4 | 0 | 6.8 |
| Propane | 15.7 ± 1.3 | 15.6 ± 1.1 | 0 | 4.1 |
| Propylene | 12.0 ± 0.2 | 14.7 ± 0.3 | 0 | 3.2 |
| $C_4$ paraffins | 5.3 ± 0.0 | 8.6 ± 0.8 | 0 | 11.5 |
| $C_4$ olefins | 2.1 ± 0.0 | 2.4 ± 0.2 | 0 | 5.6 |
| $C_5$ paraffins | 0.5 ± 0.0 | 0.8 ± 0.0 | 0 | 0.2 |
| $C_5$ olefins | 0.4 ± 0.0 | 0.4 ± 0.0 | 0 | 0.3 |
| Benzene | 7.9 ± 0.5 | 5.2 ± 0.4 | 13.2 ± 1.1 | 4.8 |
| Toluene | 12.0 ± 1.0 | 8.0 ± 0.7 | 0 | 7.4 |
| Xylene | 4.8 ± 0.5 | 2.2 ± 0.2 | 10.9 ± 0.5 | 10.8 |
| Unidentified carbons | 7.8 ± 2.9 | 7.7 ± 4.1 | 0 | 14.8 |
| Coke | 0.20 | 0.07 | 0.3 | – |
| Carbon balance (%) | 87.1 | 85.4 | 96.1 | 72 |
| Hydrogen yield (%) | 1.5 ± 0.1 | 1.4 ± 0.1 | 0 | – |
| ***Overall selectivity (%)*** | | | | |
| Paraffins | 34.8 | 42.2 | 0 | 25.9 |
| Olefins | 27.6 | 30.1 | 0 | 22.1 |
| Aromatics | 28.4 | 18.7 | 98.8 | 20.8 |
| Unidentified carbon | 9.0 | 8.9 | 0 | 20.8 |
| Coke | 0.2 | 0.1 | 1.2 | – |
| ***Paraffin selectivity (%)*** | | | | |
| Methane | 16.7 | 13.5 | 0 | 8.9 |
| Ethane | 12.3 | 17.6 | 0 | 5.5 |
| Propane | 51.8 | 43.0 | 0 | 22.0 |
| C4 paraffins | 17.5 | 23.8 | 0 | 62.6 |
| C5 paraffins | 1.7 | 2.1 | 0 | 1.9 |
| ***Olefin selectivity (%)*** | | | | |
| Ethylene | 40.0 | 32.3 | 0 | 43 |
| Propylene | 49.8 | 57.0 | 0 | 20.2 |
| C4 olefins | 8.5 | 9.1 | 0 | 35.4 |
| C5 olefins | 1.6 | 1.6 | 0 | 1.4 |
| ***BTX selectivity (%)*** | | | | |
| Benzene | 32.2 | 34 | 54.8 | 33.6 |
| Toluene | 48.4 | 52 | – | 49 |
| Xylene | 19.4 | 14 | 45.2 | 13.7 |

Zeolites with small and medium pore sizes increase the selectivity towards light olefins and aromatics while large pore zeolites can process bulky feedstocks such as crude oil and plastic [37,38]. Notably, of the

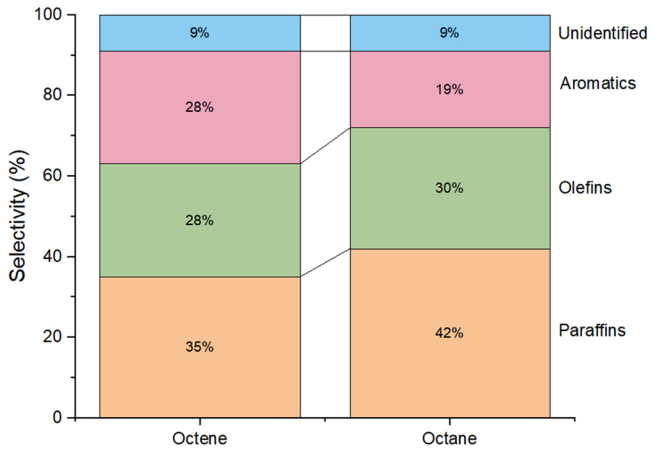


**Fig. 2.** Product distribution from cracking 1-octene and octane (reaction conditions: $m_{ZSM-5}$ = 1000 mg, 500 °C, $P_{1\text{-}octene}$ = 4 kPa, $N_2$ = 140 mL min$^{-1}$, contact time = 1.0 s).

studied medium-pore zeolites, ZSM-5 has been shown to have the highest yield of aromatics as its topology allows the formation of transition states leading to BTX [37,39,40]. In addition to the formation of aromatics, the reaction also yields paraffins and coke. Several groups have proposed that these secondary products originate from hydrogen transfer, Diels-Alder and aromatization reactions [41–44]. One way to verify the reaction network is by changing the contact time, which has been used to identify key intermediates in methanol-to-olefin chemistry [45,46]. By increasing the contact time systematically, the order at which the product appears can reveal the reaction network. Despite the large number of empirical studies looking at plastic pyrolysis and catalytic upgrading, a fundamental study investigating the cracking reaction network of key model compounds is lacking [8,11,47–49]. The objective of this paper is to study the reaction mechanism and chemistry for cracking of 1-octene, octane, toluene and octadiene on ZSM-5. These model compounds represent the major components in a plastic pyrolysis oil [6,9].

## 2. Experimental section

### 2.1. Materials

n-Octane (anhydrous, 99 %), 1-octene (98 %), 1,7-octadiene (98 %), and toluene (anhydrous, 99.8 %) (Sigma-Aldrich) were used without any pretreatment. ZSM-5 (CBV 3024E, Zeolyst International, $SiO_2/Al_2O_3$ = 30) was used as the catalyst. pXRD, surface area and pore measurement are reported (Appendix A Supplementary data). The HZSM-5 catalyst was sieved to 425–600 μm before reaction. The catalyst was calcined at 600 °C (ramp rate of 1 °C/minute) for under 100 mL min$^{-1}$ air (dry air, Airgas) for 3 h prior to reaction. Eqs. 1–8 were used to calculate the yield, selectivity, contact time and turnover numbers reported in this paper. The density of ZSM-5 used to calculate contact time in this paper is 0.5 g mL$^{-1}$. Error bars in the figures are based on the standard deviation from three measurements during steady state.

$$Hydrocarbon\ yield(\%) = \frac{moles\ of\ carbon\ in\ a\ product}{moles\ of\ carbon\ enters\ the\ reactor} * 100 \quad (1)$$

$$Overall\ selectivity(\%) = \frac{moles\ of\ carbon\ in\ a\ product\ group}{moles\ of\ carbon\ in\ all\ products} * 100 \quad (2)$$

$$Paraffin\ selectivity(\%) = \frac{moles\ of\ carbon\ in\ a\ paraffin\ product}{moles\ of\ carbon\ in\ all\ paraffin\ products} * 100 \quad (3)$$

$$Olefin\ selectivity(\%) = \frac{moles\ of\ carbon\ in\ an\ olefin\ product}{moles\ of\ carbon\ in\ all\ olefin\ products} * 100 \quad (4)$$

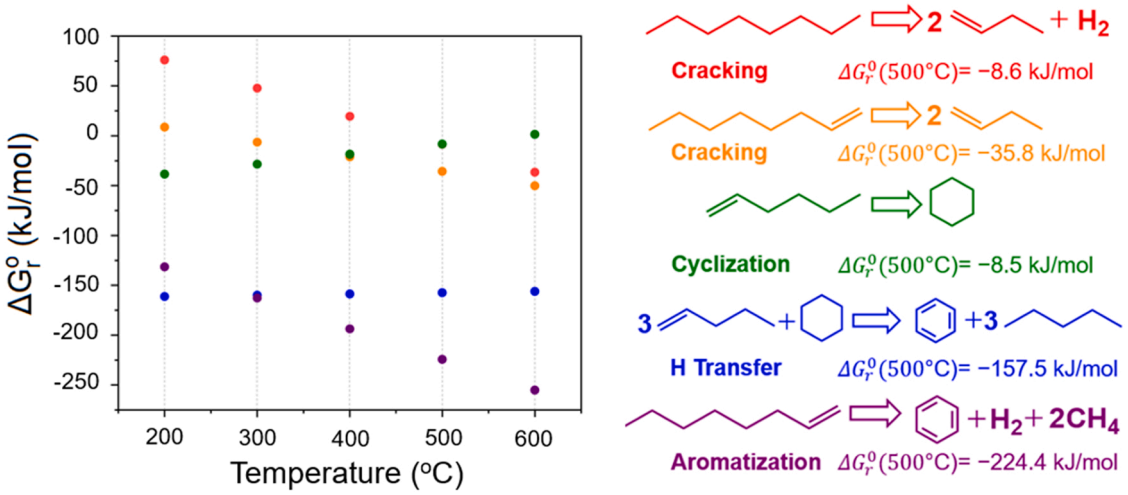


**Fig. 3.** Gibbs free energy as a function of temperature of cracking reactions.

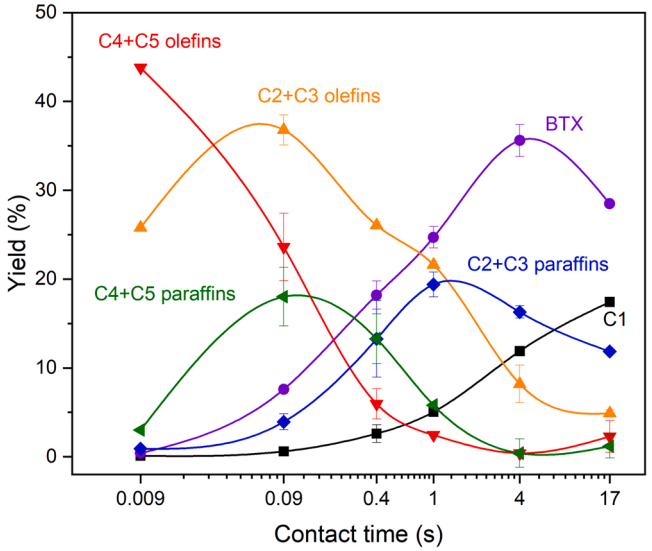


**Fig. 4.** Grouped products from cracking 1-octene (reaction conditions: $m_{ZSM\text{-}5}$ = 10–20000 mg, 500 °C, 4kPa of octene, $N_2$ = 140 mL $min^{-1}$, contact time = 0.009–17 s). Error bars are based on the standard deviation from three data points during steady state.

$$Aromatics\ selectivity(\%) = \frac{moles\ of\ carbon\ in\ an\ aromatic\ product}{moles\ of\ carbon\ in\ all\ aromatic\ products} * 100 \quad (5)$$

$$Contact\ time(s) = \frac{volume\ of\ catalyst\ (mL)}{total\ volumetric\ flow\ \left(\frac{mL}{min}\right)} \quad (6)$$

$$Hydrogen\ yield(\%) = \frac{moles\ of\ hydrogen\ in\ H_2}{moles\ of\ hydrogen\ in\ the\ reactant} * 100 \quad (7)$$

$$Carbon\ balance(\%) = \frac{moles\ of\ carbon\ in\ all\ products}{moles\ of\ carbon\ enters\ the\ reactor} * 100 \quad (8)$$

Mesoporous ZSM-5 was synthesized by desilication of ZSM-5 (CBV 3024E, Zeolyst International, $SiO_2/Al_2O_3$ = 30) using a modified method reported by Jensen and coworkers [50]. 20 g zeolite (ammonium form) was desilicated with 0.6 M NaOH for 30 min at 65 °C in a round bottom flash (liquid to solid ratio of 50). The solution was quickly cooled by an ice bath. The solid was filtered and washed with 18.2 MΩ water. The solid was then dried overnight in an oven at 120 °C followed by acid washing with 0.06 M HCl solution for 6 h at 65 °C. The solid was filtered and washed with 18.2 MΩ water. The hierarchical material was ion-exchanged with 1 M $NH_4NO_3$ at 80 °C for 24 h, dried overnight and then calcined at 550 °C (ramp 1 °C/min) for 5 h under dry air flow. pXRD, pore (Ar physisorption) and acid site (ammonia temperature programmed desorption) measurements of the final material are reported in Appendix A Supplementary data.

### 2.2. Catalytic measurements

The catalytic reactions were carried out in a fixed-bed quartz tube reactor of ½ inch outer diameter with a quartz frit. Sieved ZSM-5 was loaded into the reactor, held by the quartz frit, and calcined as describe above. The reactor temperature was measured using a K-type thermocouple located at the quartz frit. The reactor configuration is shown in Fig. S1. The temperature was then lowered to 500 °C at 10 °C $min^{-1}$, while purging the reactor with $N_2$ (140 mL $min^{-1}$) for an additional 10 min. The temperature was then further lowered to reaction temperature. The feed (one of the following: 1-octene, octane, octadiene, toluene or a mixture of 1-octene and octane) was individually introduced into an evaporator, kept at 250 °C, using a syringe pump (Fisherbrand™ Single Syringe Pump) at the rate of 0.04 mL $min^{-1}$ (or 0.0007 mL $s^{-1}$). The feed was injected continuously. The reactor was operated at ambient pressure. Liquid products were collected by a condenser, cooled by an isopropanol dry ice bath (temperature: −78 °C) while gaseous products were collected using a gas bag. Condensed products that were accumulated over 60 min were collected and diluted to 25 mL by adding isopropanol. Gas and liquid samples were collected every 60 min. Liquid and gaseous products were analyzed offline using gas chromatography (GC).

Liquid products were analyzed and quantified with a GC-FID (Shimadzu 2014) equipped with an RTX-VMS column (Restek). The calibration of C4-C20 hydrocarbons, BTX, and other aromatics signals used C8-C20 standard (Sigma-Aldrich) and 1000 ppm solutions that were made by dissolving analytes in isopropanol. Gas products were analyzed using a Refinery Gas Analyzer GC-2014 (Shimadzu) with 1) Restek RTX–alumina column and an FID to analyze C1–C5 hydrocarbons and 2) RTX-Q-plot column and RTX-MS-5A column with a thermal conductivity detector (TCD) to quantify $H_2$, respectively. The GC signal was calibrated with a commercial calibration mixture containing C1-C6 *n*-paraffins, C2-C6 olefins, and $H_2$ standards (Scott Gas, 1000 ppm of each hydrocarbon and 10000 ppm $H_2$).

**Table 2**
1-Octene cracking products at different contact times.

| Contact time (s) | 0.009 | 0.09 | 0.4 | 1 | 4 | 17 |
|---|---|---|---|---|---|---|
| 1-Octene conversion | 88 | 100 | 100 | 100 | 100 | 100 |
| ***Yield (%)*** | | | | | | |
| Methane | 0.1 ± 0.0 | 0.6 ± 0.0 | 2.6 ± 1.0 | 5.1 ± 0.1 | 11.9 ± 0.1 | 17.4 ± 0.2 |
| Ethane | 0.4 ± 0.1 | 0.4 ± 0.1 | 1.6 ± 0.6 | 3.7 ± 0.4 | 5.3 ± 0.1 | 7.3 ± 0.1 |
| Ethylene | 4.4 ± 0.1 | 12.6 ± 0.5 | 10.7 ± 3.9 | 9.6 ± 0.4 | 4.0 ± 0.1 | 2.6 ± 0.1 |
| Propane | 0.5 ± 0.0 | 3.5 ± 0.9 | 11.6 ± 4.2 | 15.7 ± 1.3 | 11.0 ± 0.7 | 4.6 ± 0.3 |
| Propylene | 21.4 ± 0.0 | 24.2 ± 1.7 | 15.3 ± 8.2 | 12.0 ± 0.2 | 4.2 ± 2.1 | 2.3 ± 0.4 |
| $C_4$ paraffins | 1.9 ± 0.1 | 15.5 ± 3.3 | 11.7 ± 2.8 | 5.3 ± 0.0 | 0.4 ± 0.0 | 1.2 ± 1.2 |
| $C_4$ olefins | 24.4 ± 0.1 | 19.1 ± 3.8 | 4.1 ± 1.0 | 2.1 ± 0.0 | 0.4 ± 0.0 | 2.1 ± 1.8 |
| $C_5$ paraffins | 1.1 ± 0.1 | 2.5 ± 0.0 | 1.6 ± 0.1 | 0.5 ± 0.0 | 0 ± 0.0 | 0.0 ± 0.0 |
| $C_5$ olefins | 19.4 ± 0.1 | 4.5 ± 0.2 | 1.9 ± 1.4 | 0.4 ± 0.0 | 0 ± 0.0 | 0.2 ± 0.1 |
| Benzene | 0.1 ± 0.0 | 1.4 ± 0.1 | 4.5 ± 0.6 | 7.9 ± 0.5 | 17.4 ± 1.1 | 18.4 ± 0.1 |
| Toluene | 0 ± 0.0 | 4.1 ± 0.2 | 9.4 ± 1.1 | 12.0 ± 1.0 | 15.2 ± 1.4 | 8.8 ± 0.1 |
| Xylene | 0.3 ± 0.0 | 2.2 ± 0.1 | 4.3 ± 1.1 | 4.8 ± 0.5 | 3.0 ± 0.1 | 1.3 ± 0.0 |
| Unidentified carbons | 2.7 ± 0.5 | 4.8 ± 1.0 | 7.6 ± 0.9 | 7.8 ± 2.9 | 12.2 ± 2.2 | 12.0 ± 1.2 |
| Coke | < 0.1 | < 0.1 | < 0.1 | 0.2 | 0.7 | 1.8 |
| Carbon balance (%) | 87.3 | 95.5 | 87 | 87.1 | 85.7 | 80 |
| Hydrogen yield (%) | 0 ± 0.0 | 0.28 ± 0.1 | 0.48 ± 0.0 | 1.5 ± 0.1 | 2.3 ± 0.2 | 2.15 ± 0.0 |
| ***Overall selectivity (%)*** | | | | | | |
| Paraffins | 4.8 | 23.6 | 33.5 | 34.7 | 33.4 | 37.0 |
| Olefins | 91.0 | 63.3 | 36.8 | 27.5 | 10.1 | 8.7 |
| Aromatics | 0.6 | 8.0 | 21.0 | 28.4 | 41.5 | 37.5 |
| Unidentified carbon | 3.6 | 5.1 | 8.6 | 9.2 | 14.2 | 14.7 |
| Coke | < 0.1 | < 0.1 | 0.1 | 0.2 | 0.8 | 2.1 |
| ***Paraffin selectivity (%)*** | | | | | | |
| Methane | 3.1 | 2.7 | 8.9 | 16.7 | 41.6 | 57.2 |
| Ethane | 2.6 | 2.0 | 5.6 | 12.3 | 18.5 | 23.9 |
| Propane | 13.6 | 15.5 | 39.9 | 51.8 | 38.4 | 15.0 |
| C4 paraffins | 51.6 | 68.5 | 40.0 | 17.5 | 1.4 | 3.9 |
| C5 paraffins | 29.1 | 11.3 | 5.6 | 1.7 | 0.1 | 0 |
| ***Olefin selectivity (%)*** | | | | | | |
| Ethylene | 6.3 | 20.8 | 33.5 | 40.0 | 46.2 | 36.5 |
| Propylene | 30.8 | 40.1 | 47.9 | 49.8 | 48.7 | 31.8 |
| C4 olefins | 35.0 | 31.6 | 12.7 | 8.5 | 4.8 | 28.7 |
| C5 olefins | 27.9 | 7.5 | 5.9 | 1.7 | 0.3 | 3.0 |
| ***BTX selectivity (%)*** | | | | | | |
| Benzene | 36.1 | 17.8 | 24.9 | 32.2 | 49.0 | 64.4 |
| Toluene | 0 | 53.4 | 51.4 | 48.4 | 42.6 | 30.9 |
| Xylene | 63.9 | 28.8 | 23.7 | 19.4 | 8.4 | 4.7 |

### 2.3. Coke quantification

The amount of coke deposited on spent catalysts was analyzed using Thermo-Gravimetric Analysis (TGA). 20 mg of spent catalyst was loaded into an aluminum pan, dried under dry air at 100 $^{o}$C for 30 min. Temperature ramped from 100 to 700 $^{o}$C at 10 $^{o}$C min$^{-1}$. The weight loss due to the burning of coke was quantified.

### 2.4. Leaching experiment

The spent catalyst was extracted with dichloromethane (DCM) overnight to selectively extract hydrocarbons without dissolving the ZSM-5 framework. GC-MS analysis of this sample was compared with a sample where the spent catalyst was digested in hydrofluoric acid (HF) and the organic compounds extracted to DCM. The undissolved hard coke was filtered.

## 3. Results and discussion

### 3.1. Stability of ZSM-5 in cracking 1-octene

The stability of ZSM-5 was tested at 80 % 1-octene conversion (500 °C) over 70 h on stream (corresponding to about 7400 g octene converted per gram ZSM-5) as shown in Fig. 1. The 1-octene conversion continuously decreased as the catalyst covers with coke. Notably, C2-C3 olefins decreased after 12 h on stream, possibly due to deactivation [51]. The performance of the catalyst in other experiments in this paper was evaluated in the first 6 h of time-on-stream to ensure less than 10 % deactivation. Additionally, the reaction was done at 500 °C since high temperature (>600 °C) led to homogeneous (gas phase) reactions with 1-octene (Fig. S2).

### 3.2. Product distributions of cracking model compounds

The cracking of each plastic oil model compound (octane, 1-octene, octadiene, toluene) was studied at long contact time (1.0 s, $m_{ZSM\text{-}5} = 1$ g) to understand the possible primary and secondary products at high conversion (Table 1). Toluene disproportionates to benzene and xylenes. The main groups of products from octane/octene include olefin, paraffins, BTX and coke. Octane, 1-octene and octadiene converted completely while only 25.4 % of toluene was converted at this contact time. The selectivity of paraffins and olefins are 9 % higher while the selectivity to BTX is 5 % higher when 1-octene is the feedstock instead of octane (Table 1, Fig. 2). Although 1,7-octadiene was clogging up the evaporator and prevented continuation of reaction after only 1.5 h (Table 1) leading to low carbon balance, the product distribution is similar to that of 1-octene. Given the low carbon balance of 72 %, this number should be interpreted with caution. We ascribe this to octadiene undergoing thermal coking at these conditions. This suggests that a more unsaturated plastic oil feedstock can produce more BTX at the same contact time compared to an alkane-rich feed like naphtha. This hypothesis is in line with our observation of an increase in signal of $m/z$ fragment 91 and 105, stemming from aromatics, in TGA-MS when 1-octene and octadiene were cracked, compared to octane (Figs. S4–5). Since a major portion of plastic oil are olefins, we examine the cracking mechanism of 1-octene in the next section.

### 3.3. Reaction network of 1-octene conversion

The thermodynamic parameters for several possible reactions (obtained from APV121. PURE37 databank) at 500 °C and 1 atm were determined using the Aspen Plus software package (version 11). In Table S1, we summarize the reactions involved in the conversion of octane, 1-octene, and octadiene over ZSM-5, including cracking, cyclization, hydrogen transfer and aromatization. At 500 °C, all these reaction pathways are thermodynamically favorable (Fig. 3). In addition, the thermodynamics of aromatization and cracking reactions are more favorable with increased degree of unsaturation of the feedstock (Table S1).

To understand the reaction network of the cascade reactions, 1-octene was catalytically cracked over ZSM-5 at various contact times. The products were grouped to identify the key reaction intermediates and pathways (Fig. 4). Detailed product selectivity and yields can be found in Table 2.

At short contact times (<10 ms), the 1-octene likely isomerizes to the more stable 2- and 3-octene as isomerization is fast (Fig. 4).[42] The octene then undergo C-C bond cleavage to form C3-C5 olefins. As

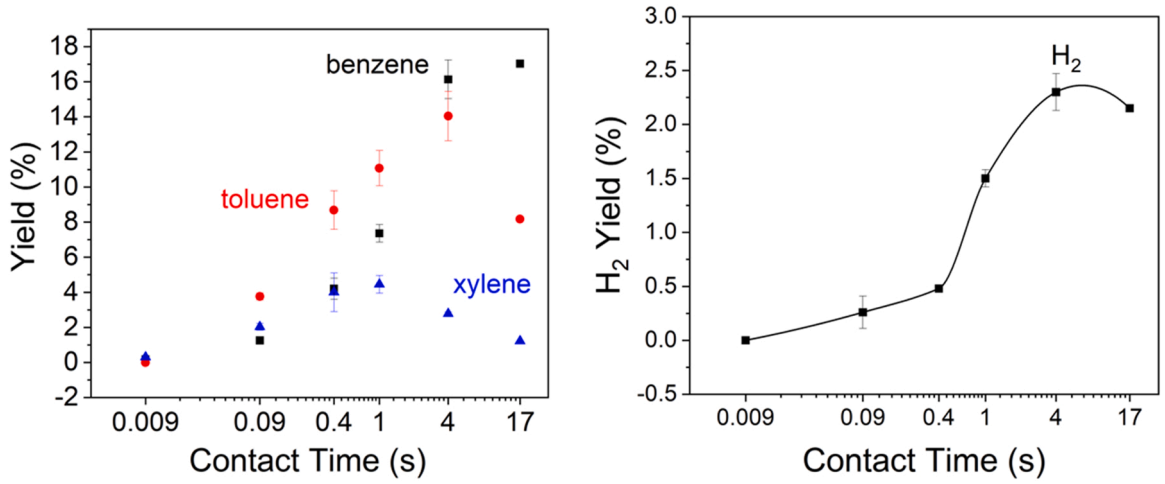


**Fig. 5.** (a) Yield of BTX, (b) $H_2$ yield at the outlet as a function of contact time (reaction conditions: $m_{ZSM\text{-}5}$ = 10–20000 mg, 500 °C, 4kPa of 1-octene, $N_2$ = 140 mL $min^{-1}$, contact time = 0.009–17 s). Error bars are based on the standard deviation from three data points during steady state.

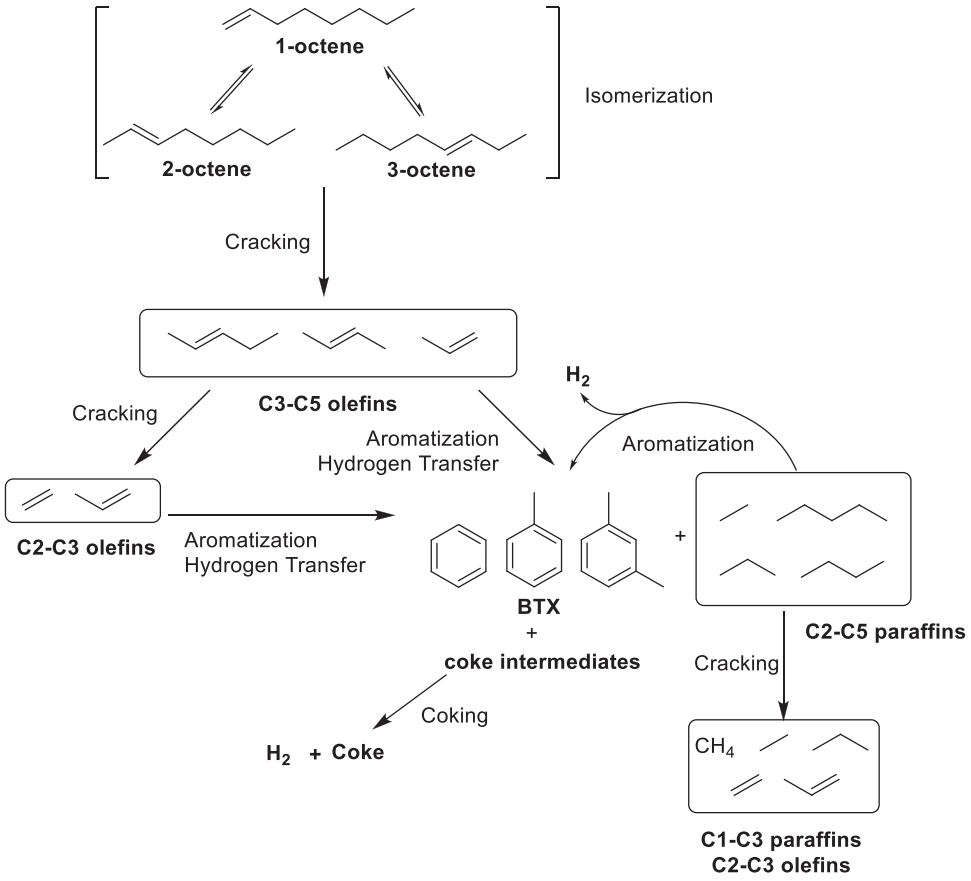


**Fig. 6.** Proposed reaction network of 1-octene over ZSM-5.

contact time increases to ~90 ms, the C4-C5 olefins decrease while the C2-C3 olefins, the C4-C5 paraffins and BTX increase. The yield of C4-C5 olefins is lower at the higher contact time, suggesting that these products could have cracked to ethylene and propylene or reacted further forming aromatics and paraffins with C2-C5 olefins via Diels-Alder and hydrogen transfer reactions. This is evidenced by the C2-C3 olefins going through a maximum, while BTX keeps increasing, indicating that C2-C5 olefins go through hydrogen transfer, cyclization, and aromatization reactions to create BTX (Fig. 5**a**). C4-C5 paraffins also reach a maximum concentration after which they decline, suggesting that these compounds can aromatize as well. C4-C5 paraffins likely undergo cracking to make shorter paraffins and olefins while also being aromatized into BTX. The similarity in C2-C3 olefins and C4-C5 paraffins suggested that the short hydrocarbons in plastic oil will eventually turn into BTX via aromatization if given enough contact time with the acidic catalyst. Additionally, with increasing contact time, an increased $H_2$ concentration (Fig. 5b) is observed, likely due to coke formation. At the longest contact time (17 s), C1-C3 paraffins, BTX, coke and $H_2$ were the major products.

At the highest contact time, benzene is the major product while toluene and xylene concentrations decrease (Fig. 5a). The

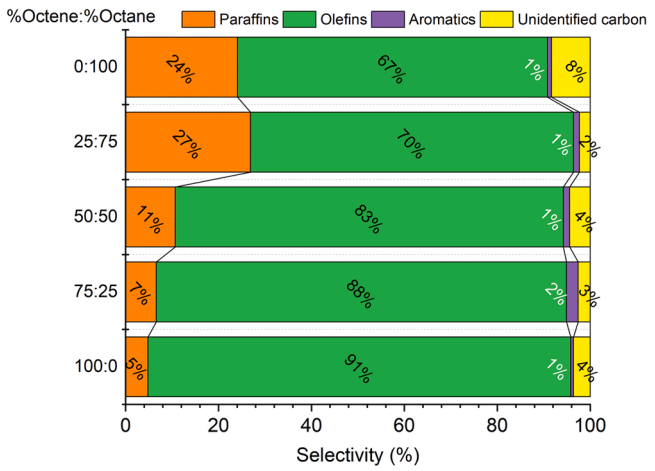


**Fig. 7.** Product selectivity from cracking mixture of octane and 1-octene (reaction conditions: $m_{ZSM\text{-}5}$ = 10 mg, 500 °C, 4 kPa of various fraction of 1-octene + octane, $N_2$ = 140 mL $min^{-1}$, contact time = 9 ms, carbon balance >85 %).

concentrations of all 3 aromatics increase from 9 to 1000 ms contact time (Fig. 5a). The size of ZSM-5 pores (5.6 Å) favors the formation of BTX from small olefins.[52] In comparison to cracking 1-octene over ZSM-5, cracking of 1-octene over silica alumina with a similar Al site density yielded 70 times less BTX (Table S3). However, the concentration of xylene decreases around a contact time of 4 s while the concentration of toluene starts to decrease around a contact time of 17 s. On the other hand, going from contact time of 4–17 s, benzene keeps increasing while toluene and xylene decrease. In addition, the higher yield of aromatics observed at the higher contact time accompanies an increase in coke yield due to an increase in aromatization activity [53, 54]. The increasing hydrogen gas concentration as a function of increasing contact time is thought to reflect increasing degrees of dehydrogenation, which ultimately lead to increasing degree of carbon retention, i.e. coking. The overall reaction network is summarized in Fig. 6. Associated with this BTX concentration change is a drop in $H_2$ yield (Fig. 5b), this is likely due to dealkylation reactions of toluene and xylene which consumed hydrogen. Since ZSM-5 is known to catalyze disproportion and dealkylation reactions, the long contact times seem to facilitate these side reactions.[55,56].

### 3.4. Cracking of mixtures of 1-octene and octane at low contact time

To better understand the combined reactivity of alkanes and olefins, various mixtures of 1-octene and octane were cracked at a contact time of 9 ms. As olefin is more reactive than paraffin, the 1-octene conversion is higher compared to conversion of octane in the mixture. At this low contact time, the yield of BTX is comparable when the feed is octane or 1-octene (Fig. 7, Table 3). Increasing degree of unsaturation of the feed can lead to more olefin yield but negligible change in BTX yield. This observation suggests that most of the aromatics resulting from cracking 1-octene did not come from direct aromatization. As indicated in the previous section, the aromatics are likely produced from Diels-Alder reactions, aromatization, and hydrogen transfer reactions between the C3-C5 hydrocarbons.

In combination with our observations in Section 3.2, we postulate that plastic oil with more unsaturated and reactive olefins would require less catalyst to be converted to BTX compared to more saturated feed. However, at a set contact time, a higher BTX yield will also lead to an increase in coke. This increase in carbon deposition could pose operational challenges to current cracking reactors if the feed were pure olefin-rich plastic oil instead of paraffin-rich naphtha.

**Table 3**
Summary of cracking mixture of octene and octane (500 °C, contact time = 9 ms and $P_{feed}$ = 4 kPa).

| Feed | Octene | 75 Octene + 25 Octane | 50 Octene + 50 Octane | 25 Octene + 75 Octane | Octane |
|---|---|---|---|---|---|
| $P_{octene}$ (kPa) | 4 | 3 | 2 | 1 | 0 |
| $P_{octane}$ (kPa) | 0 | 1 | 2 | 3 | 4 |
| Octene conversion (%) | 88.2 | 85.7 | 90.4 | 92.4 | – |
| Octane conversion (%) | – | 54.2 | 8.9 | 8.1 | 12.7 |
| ***Yield (%)*** | | | | | |
| Methane | 0.1 | 0.1 | 0.1 | 0.1 | 0.1 |
| Ethane | 0.4 | 0.2 | 0.3 | 0.5 | 0.6 |
| Ethylene | 4.4 | 3.7 | 3.5 | 3.0 | 1.7 |
| Propane | 0.5 | 0.9 | 0.7 | 1.3 | 1.0 |
| Propylene | 21.4 | 17.3 | 11.6 | 11.5 | 5.7 |
| $C_4$ paraffins | 1.9 | 1.8 | 2.4 | 5.8 | 1.9 |
| $C_4$ olefins | 24.4 | 17.3 | 14.1 | 7.7 | 3.3 |
| $C_5$ paraffins | 1.1 | 0.9 | 1.4 | 2.6 | 0.6 |
| $C_5$ olefins | 19.4 | 13.2 | 8.6 | 4.5 | 1.0 |
| Benzene | 0.1 | 0.2 | 0.2 | 0.2 | 0.1 |
| Toluene | 0 | 0.0 | 0.0 | 0.0 | 0.0 |
| Xylene | 0.3 | 0.3 | 0.4 | 0.2 | 0.1 |
| Unidentified carbons | 2.7 | 1.5 | 2.0 | 0.9 | 1.5 |
| Coke | <0.1 | <0.1 | <0.1 | <0.1 | <0.1 |
| ***Overall selectivity (%)*** | | | | | |
| Paraffins | 4.8 | 6.6 | 10.7 | 26.9 | 24.0 |
| Olefins | 91.0 | 88.4 | 83.5 | 69.6 | 66.7 |
| Aromatics | 0.6 | 2.5 | 1.4 | 1.3 | 0.9 |
| Unidentified carbon | 3.6 | 2.5 | 4.4 | 2.2 | 8.4 |
| Coke | <0.1 | <0.1 | <0.1 | <0.1 | <0.1 |
| ***Paraffin selectivity (%)*** | | | | | |
| Methane | 3.1 | 3.3 | 2.6 | 1.3 | 3.2 |
| Ethane | 2.6 | 5.0 | 6.1 | 4.6 | 14.7 |
| Propane | 13.6 | 22.7 | 13.4 | 12.2 | 23.1 |
| C4 paraffins | 51.6 | 46.2 | 49.4 | 56.5 | 45.5 |
| C5 paraffins | 29.1 | 22.8 | 28.5 | 25.4 | 13.5 |
| ***Olefin selectivity (%)*** | | | | | |
| Ethylene | 6.3 | 7.2 | 10.0 | 11.1 | 14.4 |
| Propylene | 30.8 | 33.4 | 30.5 | 43.1 | 48.9 |
| C4 olefins | 35.0 | 34.0 | 37.1 | 28.7 | 28.0 |
| C5 olefins | 27.9 | 25.4 | 22.4 | 17.1 | 8.7 |
| ***BTX selectivity (%)*** | | | | | |
| Benzene | 36.1 | 36.7 | 35.2 | 47.8 | 50.7 |
| Toluene | 0 | 0 | 0 | 0 | 0 |
| Xylene | 63.9 | 63.3 | 64.8 | 52.2 | 49.3 |

**Table 4**
Dichloromethane-soluble hydrocarbons from leaching experiments.

| | Inside pores (25.8 %) | Outside pores (74.2 %) |
|---|---|---|
| Straight alkane | $C_{10}$-$C_{20}$ = 71.1 | $C_{16}$ = 1.7 |
| Branched alkane | $C_9$-$C_{14}$ = 14.9 | $C_{10}$ = 1.0 |
| straight alkene | $C_{14}$ = 1.8 | $C_{16}$ = 1.3 |
| Branched alkene | $C_9$ = 3.2 | $C_9$-$C_{12}$ = 96.0 |
| Aromatics | $C_{11}$-$C_{15}$ = 9.0 | 0 |

### 3.5. HF dissolved species analysis

Carbon species inside the pores and on the external surface of the deactivated catalyst were investigated using leaching experiments. In

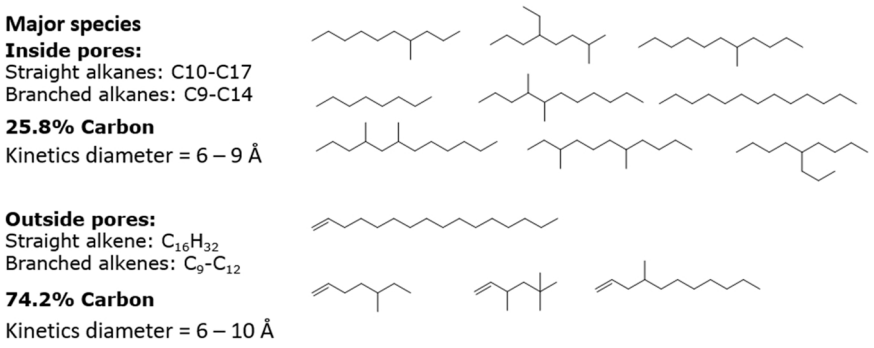


**Fig. 8.** Dichloromethane-soluble species found inside and outside of spent ZSM-5 catalysts.

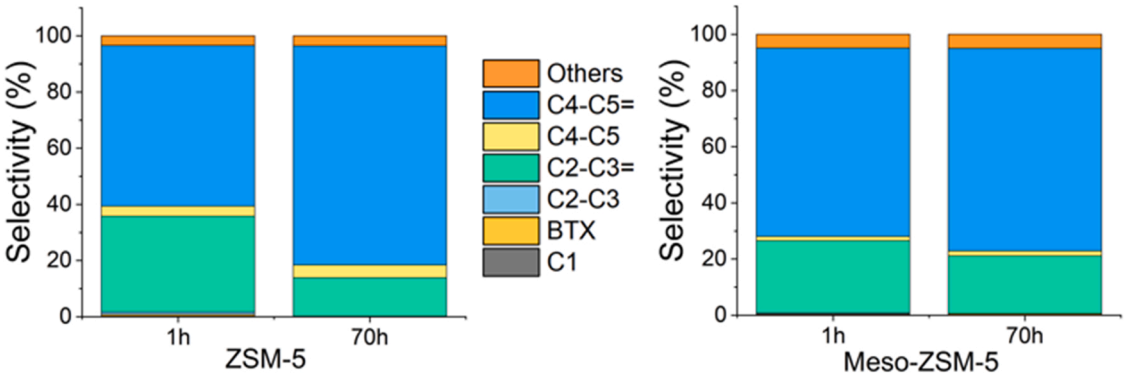


**Fig. 9.** Selectivity of products after 70 h on stream of ZSM-5 and Meso-ZSM-5. (Reaction conditions: $m_{catalyst}$ = 10 mg, 500 °C, 4kPa of 1-octene $N_2$ = 140 mL $min^{-1}$, contact time = 9 ms).

the first experiment, the spent catalyst was stirred with DCM overnight to selectively extract hydrocarbons without dissolving the ZSM-5 framework [57–62]. In a second experiment, the spent catalyst was dissolved using HF and the organic compounds extracted into DCM. The undissolved poly-aromatics (hard coke) was filtered off. The DCM solutions from both experiments were then analyzed using GC-MS. By subtracting the contribution of hydrocarbons in the first experiment from the hydrocarbons extracted in the second experiment, we can differentiate between hydrocarbons inside and outside of the framework. Table 4 summarizes the different species found from the leaching experiments. Fig. 8 illustrates the dominant species found (detailed product table can be found in Table S2). Most linear and branched alkanes can be found inside the pores, while branched alkenes are more prevalent on the external surface of the catalyst. Only a small number of substituted aromatics were observed inside the pores of the spent catalysts, indicating that monoaromatics are likely formed inside the pores but can easily diffuse out of the pores of ZSM-5, consistent with the pore openings in ZSM-5 of 5.6 Å [63]. Our observation of less than < 10 % aromatics inside the pore is in sharp contrast with the hydrogen transfer reaction in methanol-to-olefin chemistry, which is catalyzed by a hydrocarbon pool made of methyl-benzene species [64]. The undissolved heavy coke species, composed of graphitic and disordered coke can be observed by UV Raman (Fig. S13).

Combining these observations with the observed evolution of the product distribution as a function of the contact time, a reaction mechanism can be proposed. According to previous findings, due to its chain length, 1-octene (and other longer 1-olefins in plastic oil) likely undergo monomolecular cracking creating shorter olefins [65]. These olefins then participate in oligomerization to create longer olefins (>C8), catalyzed by Brønsted acid sites both inside and outside the pores of ZSM-5 [66]. As the calculated kinetic diameters of all the extracted molecules (Table S2) are higher than the diameter of the pore opening (5.6 Å), they could not diffuse in and out of the pores [67]. Inside the confinement of the pores, the hydrogen transfer between surface carbenium ions and internal long-chain olefins (>C8) at high conversions leads to the formation of hydrogen-deficient species and internal long-chain paraffins. These hydrogen deficient carbenium intermediates can go on to form BTX and coke via cyclization and hydrogen transfer [68]. Meanwhile, due to the lack of confinement effect, most of the oligomers outside the pores remained as branched and unsaturated hydrocarbons as it is more difficult for these molecules to approach an Brønsted acid site and participate in hydrogen transfer reaction. The blockage of long-chain hydrocarbons inside the pores and formation of coke on the outside of the catalyst lead to catalyst deactivation [69]. Mesopores can limit deactivation by increasing the diffusion of such bulky molecules and allow more homogeneous coke distribution [51, 70]. As shown in Table S5 and Fig. 9, although both ZSM-5 and meso-ZSM-5 experienced a decrease in 1-octene conversion after 70 h on stream, mesoporous ZSM-5 maintained product selectivity whereas conventional ZSM-5 experienced a the change in product selectivity. BTX, the final products in the cascade of reactions of 1-octene over ZSM-5, were still produced after 70 h on stream with meso-ZSM-5 (Table S5).

## 4. Conclusion

The cracking of model compounds that represent components of pyrolysis oil from plastics was studied over ZSM-5 in a continuous flow fixed-bed reactor. At 500 °C, the cracking, hydrogen transfer, cyclization, aromatization, and coking reactions are thermodynamically favorable. Contact time experiment revealed the reaction network of 1-octene over ZSM-5. At low contact time, short-chain olefins were the main products while at high contact time, aromatics, paraffins, $H_2$, coke and methane were the main products. Paraffins were produced along with the aromatics through hydrogen transfer reactions. Notably, at contact time of 0.6 s, 1-octene produced more BTX compared to octane

even though both were completely converted. This observation is in line with the increase in the aromatics signal in TGA-MS, which suggests that more unsaturated feed can favorably produce BTX. Saturated alkanes, which could have been products of hydrogen transfer reactions inside the pores, filled the pores while hard coke and unsaturated hydrocarbons remained on the outside of the catalyst structure. We observed less than 10 % aromatics inside the pores, indicating that hydrocarbon pool mechanism is unlikely facilitating reactions. Mesopores limit the deactivation, due to the increased diffusion of long chain hydrocarbons that cause pore blockages. Xylene disproportionate into toluene and benzene as well as creates coke.

## CRediT authorship contribution statement

**S Dong**: Conceptualization; Data curation; Formal analysis; Investigation; Methodology; Visualization; Roles/Writing - original draft; Writing - review & editing. **H Li**: Conceptualization; Investigation; Methodology; Roles/Writing - original draft. **IK Bloede**: Investigation; Data curation; **AJ Al Abdulghani:** Investigation; Data curation; **EA Lebrón-Rodríguez**: Investigation; Data curation; **GW Huber**: Conceptualization; Roles/Writing - original draft; Writing - review & editing; Supervision; Funding acquisition; Project administration; Resources; Writing - review & editing. **I Hermans:** Conceptualization; Roles/Writing - original draft; Writing - review & editing; Supervision; Funding acquisition; Project administration; Resources; Writing - review & editing.

## Declaration of Competing Interest

The authors declare that they have no known competing financial interests or personal relationships that could have appeared to influence the work reported in this paper.

## Data Availability

Data will be made available on request.

## Acknowledgments

This work is supported by the U.S. Department of Energy, Office of Energy Efficiency and Renewable Energy, Bioenergy Technologies Office under Award Number DE-EE0009285.

## Appendix A. Supporting information

Supplementary data associated with this article can be found in the online version at doi:10.1016/j.apcatb.2022.122219.

## References

[1] R. Geyer, J.R. Jambeck, K.L. Law, Production, use, and fate of all plastics ever made, Sci. Adv. 3 (2017), https://doi.org/10.1126/SCIADV.1700782/SUPPL_FILE/1700782_SM.PDF.
[2] X. Wang, Z. Dan, X. Cui, R. Zhang, S. Zhou, T. Wenga, B. Yan, G. Chen, Q. Zhang, L. Zhong, Contamination, ecological and health risks of trace elements in soil of landfill and geothermal sites in Tibet, Sci. Total Environ. 715 (2020), 136639, https://doi.org/10.1016/J.SCITOTENV.2020.136639.
[3] P. He, L. Chen, L. Shao, H. Zhang, F. Lü, Municipal solid waste (MSW) landfill: a source of microplastics? -evidence of microplastics in landfill leachate, Water Res. 159 (2019) 38–45, https://doi.org/10.1016/J.WATRES.2019.04.060.
[4] O. Hockman, E.G. Hwang, G. Rudzitis, Environmental costs of landfills and incinerators, (1976). https://doi.org/10.2172/7319370.
[5] H. Li, H.A. Aguirre-Villegas, R.D. Allen, X. Bai, C.H. Benson, G.T. Beckham, S. L. Bradshaw, J.L. Brown, R.C. Brown, M.A.S. Castillo, V.S. Cecon, J.B. Curley, G. W. Curtzwiler, S. Dong, S. Gaddameedi, J.E. Garcia, I. Hermans, M.S. Kim, J. Ma, L. O. Mark, M. Mavrikakis, O.O. Olafasakin, T.A. Osswald, K.G. Papanikolaou, H. Radhakrishnan, K.L. Sánchez-Rivera, K.N. Tumu, R.C. van Lehn, K.L. Vorst, M. M. Wright, J. Wu, V.M. Zavala, P. Zhou, G.W. Huber, Expanding plastics recycling technologies: chemical aspects, Technol. Status Chall. (2022), https://doi.org/10.26434/CHEMRXIV-2022-9WQZ0.
[6] D. Zhao, X. Wang, J.B. Miller, G.W. Huber, The chemistry and kinetics of polyethylene pyrolysis: a process to produce fuels and chemicals, ChemSusChem 13 (2020) 1764–1774, https://doi.org/10.1002/cssc.201903434.
[7] M. Kusenberg, A. Eschenbacher, M.R. Djokic, A. Zayoud, K. Ragaert, S. de Meester, K.M. van Geem, Opportunities and challenges for the application of post-consumer plastic waste pyrolysis oils as steam cracker feedstocks: to decontaminate or not to decontaminate? Waste Manag. 138 (2022) 83–115, https://doi.org/10.1016/J.WASMAN.2021.11.009.
[8] A. Eschenbacher, F. Goodarzi, R.J. Varghese, K. Enemark-Rasmussen, S. Kegnaes, S. Abbas-Abadi, K.M. van Geem, Boron-modified mesoporous ZSM-5 for conversion of pyrolysis vapors from LDPE and mixed polyolefins: Maximizing the C 2-C 4 olefin yield with minimal carbon footprint, n.d.
[9] M. Kusenberg, M. Roosen, A. Zayoud, M.R. Djokic, H. Dao Thi, S. de Meester, K. Ragaert, U. Kresovic, K.M. van Geem, Assessing the feasibility of chemical recycling via steam cracking of untreated plastic waste pyrolysis oils: feedstock impurities, product yields and coke formation, Waste Manag. 141 (2022) 104–114, https://doi.org/10.1016/J.WASMAN.2022.01.033.
[10] M. Kusenberg, A. Zayoud, M. Roosen, H.D. Thi, M.S. Abbas-Abadi, A. Eschenbacher, U. Kresovic, S. de Meester, K.M. van Geem, A comprehensive experimental investigation of plastic waste pyrolysis oil quality and its dependence on the plastic waste composition, Fuel Process. Technol. 227 (2022), 107090, https://doi.org/10.1016/J.FUPROC.2021.107090.
[11] A. Eschenbacher, R.J. Varghese, E. Delikonstantis, O. Mynko, F. Goodarzi, K. Enemark-Rasmussen, J. Oenema, M.S. Abbas-Abadi, G.D. Stefanidis, K.M. van Geem, Highly selective conversion of mixed polyolefins to valuable base chemicals using phosphorus-modified and steam-treated mesoporous HZSM-5 zeolite with minimal carbon footprint, Appl. Catal. B 309 (2022), 121251, https://doi.org/10.1016/J.APCATB.2022.121251.
[12] W. Kaminsky, B. Schlesselmann, C. Simon, Olefins from polyolefins and mixed plastics by pyrolysis, J. Anal. Appl. Pyrolysis 32 (1995) 19–27, https://doi.org/10.1016/0165-2370(94)00830-T.
[13] L.O. Mark, M.C. Cendejas, I. Hermans, The use of heterogeneous catalysis in the chemical valorization of plastic waste, ChemSusChem 13 (2020) 5808–5836, https://doi.org/10.1002/cssc.202001905.
[14] E. Hájeková, B. Mlynková, M. Bajus, L. Špodová, Copyrolysis of naphtha with polyalkene cracking products; the influence of polyalkene mixtures composition on product distribution, J. Anal. Appl. Pyrolysis 79 (2007) 196–204, https://doi.org/10.1016/J.JAAP.2006.12.022.
[15] L.D. Ellis, N.A. Rorrer, K.P. Sullivan, M. Otto, J.E. McGeehan, Y. Román-Leshkov, N. Wierckx, G.T. Beckham, Chemical and biological catalysis for plastics recycling and upcycling, Nat. Catal. 4 (2021) 539–556, https://doi.org/10.1038/S41929-021-00648-4.
[16] Anellotech says Plas-TCat is a game-changer | Sustainable Plastics, (n.d.). ⟨https://www.sustainableplastics.com/news/anellotech-says-plas-tcat-game-changer⟩ (accessed May 18, 2022).
[17] Bio-TCatTM for Renewable Chemicals & Fuels | Anellotech, Inc | Cost Competitive Bio-Sourced Chemicals and Fuels, (n.d.). ⟨https://anellotech.com/bio-tcat⟩ (accessed July 6, 2022).
[18] Suntory Introduces 100% Plant-Based PET Bottle Prototypes | Business Wire, (n.d.). ⟨https://www.businesswire.com/news/home/20211202005948/en/Suntory-Introduces-100-Plant-Based-PET-Bottle-Prototypes⟩ (accessed July 6, 2022).
[19] A.G. Stepanov, A.A. Shubin, M. v Luzgin, H. Jobic, A. Tuel, Molecular dynamics of n-octane inside zeolite ZSM-5 as studied by deuterium solid-state nmr and quasi-elastic neutron scattering, J. Phys. Chem. B 102 (1998) 10860–10870, https://doi.org/10.1021/JP982790T.
[20] C.S. Triantafillidis, N.P. Evmiridis, L. Nalbandian, I.A. Vasalos, Performance of ZSM-5 as a fluid catalytic cracking catalyst additive: effect of the total number of acid sites and particle size, Ind. Eng. Chem. Res 38 (1999) 916–927, https://doi.org/10.1021/IE980395J.
[21] S. Altwasser, C. Welker, Y. Traa, J. Weitkamp, Catalytic cracking of n-octane on small-pore zeolites, Microporous Mesoporous Mater. 83 (2005) 345–356, https://doi.org/10.1016/J.MICROMESO.2005.04.028.
[22] C. Liu, Y. Deng, Y. Pan, Y. Gu, B. Qiao, X. Gao, Effect of ZSM-5 on the aromatization performance in cracking catalyst, J. Mol. Catal. A Chem. 215 (2004) 195–199, https://doi.org/10.1016/J.MOLCATA.2004.02.001.
[23] X. Xiao, B. Sun, P. Wang, X. Fan, L. Kong, Z. Xie, B. Liu, Z. Zhao, Tuning the density of Brønsted acid sites on mesoporous ZSM-5 zeolite for enhancing light olefins selectivity in the catalytic cracking of n-octane, Microporous Mesoporous Mater. 330 (2022), 111621, https://doi.org/10.1016/J.MICROMESO.2021.111621.
[24] N.G. Grigor'eva, S. v Bubennov, B.I. Kutepov, Oligomerization of α-octene catalyzed by zeolites, 2011 3:2, Catal. Ind. 3 (2011) 144–150, https://doi.org/10.1134/S207005041102019X.
[25] N.G. Grigor'eva, S. v Bubennov, B.I. Kutepov, Oligomerization of α-octene catalyzed by zeolites, 2011 3:2, Catal. Ind. 3 (2011) 144–150, https://doi.org/10.1134/S207005041102019X.
[26] L. Zhang, H. Zhang, Z. Chen, Q. Ning, S. Liu, J. Ren, X. Wen, Y.W. Li, Insight into the impact of Al distribution on the catalytic performance of 1-octene aromatization over ZSM-5 zeolite, Catal. Sci. Technol. 9 (2019) 7034–7044, https://doi.org/10.1039/C9CY01672D.
[27] P. Liu, Z. Zhang, M. Jia, X. Gao, J. Yu, ZSM-5 zeolites with different SiO2/Al2O3 ratios as fluid catalytic cracking catalyst additives for residue cracking, Chin. J. Catal. 36 (2015) 806–812, https://doi.org/10.1016/S1872-2067(14)60311-9.
[28] J.S. Buchanan, Gasoline selective ZSM-5 FCC additives: model reactions of C6–C10 olefins over steamed 55:1 and 450:1 ZSM-5, Appl. Catal. A Gen. 171 (1998) 57–64, https://doi.org/10.1016/S0926-860X(98)00074-X.

[29] V.S. Nayak, J.B. Moffat, Effect of silicon-to-aluminum ratio and template on the cracking of C6—8 alkenes over ZSM-5 zeolite, Appl. Catal. 60 (1990) 87–99, https://doi.org/10.1016/S0166-9834(00)82174-0.
[30] H. Long, X. Wang, W. Sun, Study of n-octene aromatization over nanoscale HZSM-5 zeolite, Microporous Mesoporous Mater. 119 (2009) 18–22, https://doi.org/10.1016/J.MICROMESO.2008.09.032.
[31] A. de Klerk, Oligomerization of 1-hexene and 1-octene over solid acid catalysts, Ind. Eng. Chem. Res. 44 (2005) 3887–3893, https://doi.org/10.1021/IE0487843.
[32] H. Long, X. Wang, W. Sun, G. Xiong, K. Wang, Effect of acidity on n-octene reaction over potassium modified nanoscale HZSM-5, Fuel 87 (2008) 3660–3663, https://doi.org/10.1016/J.FUEL.2008.06.007.
[33] H. Long, X. Wang, W. Sun, X. Guo, Conversion of n-octene over nanoscale HZSM-5 zeolite, Catal. Lett. 126 (2008) 378–382, https://doi.org/10.1007/S10562-008-9636-9/FIGURES/6.
[34] J.S. Buchanan, J.G. Santiesteban, W.O. Haag, Mechanistic considerations in acid-catalyzed cracking of olefins, J. Catal. 158 (1996) 279–287, https://doi.org/10.1006/JCAT.1996.0027.
[35] J.S. Buchanan, D.H. Olson, S.E. Schramm, Gasoline selective ZSM-5 FCC additives: effects of crystal size, SiO2/Al2O3, steaming, and other treatments on ZSM-5 diffusivity and selectivity in cracking of hexene/octene feed, Appl. Catal. A Gen. 220 (2001) 223–234, https://doi.org/10.1016/S0926-860X(01)00712-8.
[36] J.S. Jung, T.J. Kim, G. Seo, Catalytic cracking of n-octane over zeolites with different pore structures and acidities, 2004 21:4, Korean J. Chem. Eng. 21 (2004) 777–781, https://doi.org/10.1007/BF02705520.
[37] V. Blay, B. Louis, T. Yokoi, K.A. Peccatiello, M. Clough, B. Yilmaz, Engineering Zeolites for Catalytic Cracking to Light Olefins, (2017). https://doi.org/10.1021/acscatal.7b02011.
[38] J.S. Buchanan, The chemistry of olefins production by ZSM-5 addition to catalytic cracking units, Catal. Today 55 (2000) 207–212, https://doi.org/10.1016/S0920-5861(99)00248-5.
[39] D. Bhattacharya, S. Sivasanker, A comparison of aromatization activities of the medium pore zeolites, ZSM-5, ZSM-22, and Eu-1, J. Catal. 153 (1995) 353–355, https://doi.org/10.1006/JCAT.1995.1137.
[40] A. Chatterjee, D. Bhattacharya, M. Chatterjee, T. Iwasaki, Suitability of using ZSM-5 over other medium pore zeolites for n-hexane aromatization — a density functional study, Microporous Mesoporous Mater. 32 (1999) 189–198, https://doi.org/10.1016/S1387-1811(99)00106-7.
[41] M. Shibata, H. Ki Tagawa, Y. Sendoda, Transformation of Propene into Aromatic Hydrocarbons over ZSM-5 Zeolites, (n.d.). https://doi.org/10.1016/S0167–2991(09)60939–3.
[42] Y. Ono, H. Kitagawa, Y. Sendoda, Transformation of But-1-ene into aromatic hydrocarbons over ZSM-5 zeolites, J. Chem. Soc., Faraday Trans. I. 83 (1987) 2913–2923.
[43] A.P. Hawkins, A. Zachariou, S.F. Parker, P. Collier, R.F. Howe, D. Lennon, Studies of propene conversion over H-ZSM-5 demonstrate the importance of propene as an intermediate in methanol-to-hydrocarbons chemistry, Catal. Sci. Technol. 11 (2021) 2924–2938, https://doi.org/10.1039/D1CY00048A.
[44] Y. Ono, H. Kitagawa, Y. Sendoda, Transformation of lower alkanes into aromatic hydrocarbons over Zsm-5 zeolites, J. Jpn. Pet. Inst. 30 (1987) 77–88, https://doi.org/10.1627/JPI1958.30.77.
[45] M.R. Gogate, Methanol-to-olefins process technology: current status and future prospects, Https://Doi.Org/10.1080/10916466.2018.1555589. 37 (2019) 559–565. https://doi.org/10.1080/10916466.2018.1555589.
[46] C.D. Chang, A.J. Silvestri, The conversion of methanol and other O-compounds to hydrocarbons over zeolite catalysts, J. Catal. 47 (1977) 249–259, https://doi.org/10.1016/0021-9517(77)90172-5.
[47] J.A. Onwudili, C. Muhammad, P.T. Williams, Influence of catalyst bed temperature and properties of zeolite catalysts on pyrolysis-catalysis of a simulated mixed plastics sample for the production of upgraded fuels and chemicals, J. Energy Inst. 92 (2019) 1337–1347, https://doi.org/10.1016/j.joei.2018.10.001.
[48] D. Yao, Y. Zhang, P.T. Williams, H. Yang, H. Chen, Co-production of hydrogen and carbon nanotubes from real-world waste plastics: Influence of catalyst composition and operational parameters, Appl. Catal. B 221 (2018) 584–597, https://doi.org/10.1016/j.apcatb.2017.09.035.
[49] Y. Xue, P. Johnston, X. Bai, Effect of catalyst contact mode and gas atmosphere during catalytic pyrolysis of waste plastics, Energy Convers. Manag. 142 (2017) 441–451, https://doi.org/10.1016/j.enconman.2017.03.071.
[50] A. Eschenbacher, P.A. Jensen, U.B. Henriksen, J. Ahrenfeldt, S. Ndoni, C. Li, J. Ø. Duus, U.V. Mentzel, A.D. Jensen, Catalytic deoxygenation of vapors obtained from ablative fast pyrolysis of wheat straw using mesoporous HZSM-5, Fuel Process. Technol. 194 (2019), 106119, https://doi.org/10.1016/J.FUPROC.2019.106119.
[51] F. Schmidt, C. Hoffmann, F. Giordanino, S. Bordiga, P. Simon, W. Carrillo-Cabrera, S. Kaskel, Coke location in microporous and hierarchical ZSM-5 and the impact on the MTH reaction, J. Catal. 307 (2013) 238–245, https://doi.org/10.1016/J.JCAT.2013.07.020.
[52] K. Yang, F. Zhou, H. Ma, C. Liu, F. Ma, G. Wu, Preparation of nanocrystalline ZSM-5 and its catalytic performance in fast pyrolysis of cellulose to produce aromatic hydrocarbons, Microporous Mesoporous Mater. 331 (2022), 111679, https://doi.org/10.1016/J.MICROMESO.2022.111679.
[53] R. Javaid, K. Urata, S. Furukawa, T. Komatsu, Factors affecting coke formation on H-ZSM-5 in naphtha cracking, Appl. Catal. A Gen. 491 (2015) 100–105, https://doi.org/10.1016/J.APCATA.2014.12.002.
[54] G. Mei Chen, X. Wen Zhang, Z. Tao Mi, Effects of pressure on coke and formation of its precursors during catalytic cracking of toluene over USY catalyst, J. Fuel Chem. Technol. 35 (2007) 211–216, https://doi.org/10.1016/S1872-5813(07)60018-8.
[55] S.A. Ali, K.E. Ogunronbi, S.S. Al-Khattaf, Kinetics of dealkylation–transalkylation of C9 alkyl-aromatics over zeolites of different structures, Chem. Eng. Res. Des. 91 (2013) 2601–2616, https://doi.org/10.1016/J.CHERD.2013.04.014.
[56] H.P.R. Oger, C.T. O'Connor, The reaction network in the conversion of 1,2,4-trimethylbenzene over HZSM-5, J. Catal. 176 (1998) 68–75.
[57] M. Guisnet, L. Costa, F.R. Ribeiro, Prevention of zeolite deactivation by coking, J. Mol. Catal. A Chem. 305 (2009) 69–83, https://doi.org/10.1016/J.MOLCATA.2008.11.012.
[58] M. Guisnet, P. Magnoux, Organic chemistry of coke formation, Appl. Catal. A Gen. 212 (2001) 83–96, https://doi.org/10.1016/S0926-860X(00)00845-0.
[59] P. Magnoux, P. Roger, C. Canaff, V. Fouche, N.S. Gnep, M. Guisnet, New technique for the characterization of carbonaceous compounds responsible for zeolite deactivation, Stud. Surf. Sci. Catal. 34 (1987) 317–330, https://doi.org/10.1016/S0167-2991(09)60370-0.
[60] M. Guisnet, P. Magnoux, Coking and deactivation of zeolites: influence of the pore structure, Appl. Catal. 54 (1989) 1–27, https://doi.org/10.1016/S0166-9834(00)82350-7.
[61] M. Guisnet, P. Magnoux, Fundamental description of deactivation and regeneration of acid zeolites, Stud. Surf. Sci. Catal. 88 (1994) 53–68, https://doi.org/10.1016/S0167-2991(08)62729-9.
[62] M. Guisnet, P. Magnoux, D. Martin, Roles of acidity and pore structure in the deactivation of zeolites by carbonaceous deposits, Stud. Surf. Sci. Catal. 111 (1997) 1–19, https://doi.org/10.1016/S0167-2991(97)80138-3.
[63] R. Roque-Malherbe, R. Wendelbo, A. Mifsud, A. Corma, Diffusion of aromatic hydrocarbons in H-ZSM-5, H-beta, and H-MCM-22 zeolites, J. Phys. Chem. 99 (1995) 14064–14071, https://doi.org/10.1021/J100038A043/ASSET/J100038A043.FP.PNG_V03.
[64] S. Müller, Y. Liu, F.M. Kirchberger, M. Tonigold, M. Sanchez-Sanchez, J.A. Lercher, Hydrogen transfer pathways during zeolite catalyzed methanol conversion to hydrocarbons, J. Am. Chem. Soc. 138 (2016) 15994–16003, https://doi.org/10.1021/JACS.6B09605/SUPPL_FILE/JA6B09605_SI_001.PDF.
[65] J. Abbot, B.W. Wojciechowski, The mechanism of catalytic cracking of n-alkenes on ZSM-5 zeolite, Can. J. Chem. Eng. 63 (1985) 462–469, https://doi.org/10.1002/CJCE.5450630315.
[66] R.J. Quann, L.A. Green, S.A. Tabak, F.J. Krambeck, Chemistry of olefin oligomerization over zsm-5 catalyst, Ind. Eng. Chem. Res 27 (1988) 565–570, https://doi.org/10.1021/IE00076A006/ASSET/IE00076A006.FP.PNG_V03.
[67] MFI: Framework Type, (n.d.). ⟨https://asia.iza-structure.org/IZA-SC/framework.php?STC=MFI⟩ (accessed July 17, 2022).
[68] A. Corma, A. v Orchillés, Current views on the mechanism of catalytic cracking, Microporous Mesoporous Mater. 35–36 (2000) 21–30, https://doi.org/10.1016/S1387-1811(99)00205-X.
[69] K. Barbera, S. Sorensen, S. Bordiga, J. Skibsted, H. Fordsmand, P. Beato, T.V. W. Janssens, Role of internal coke for deactivation of ZSM-5 catalysts after low temperature removal of coke with NO 2, Catal. Sci. Technol. 2 (2012) 1196–1206, https://doi.org/10.1039/C2CY00529H.
[70] J.C. Groen, W. Zhu, S. Brouwer, S.J. Huynink, F. Kapteijn, J.A. Moulijn, J. Pérez-Ramírez, Direct demonstration of enhanced diffusion in mesoporous ZSM-5 zeolite obtained via controlled desilication, J. Am. Chem. Soc. 129 (2007) 355–360, https://doi.org/10.1021/ja065737o.